Article

Classification of cotton water stress using convolutional neural networks and UAV-based RGB imagery

Haoyu Niu[1,*], Juan Landivar[2], Nick Duffield[1]

[1] Department of Electrical & Computer Engineering, Texas A&M Institute of Data Science and Texas A&M University, College Station 77843, Texas, United States

[2] Texas A&M AgriLife Research and Extension Center, Corpus Christi 78406, Texas, United States

* Corresponding author: Haoyu Niu, hniu@tamu.edu

Abstract: Embracing smart irrigation management techniques empowers growers to irrigate with greater efficiency, thereby promoting sustainable agricultural production. In this context, growers often rely on crop evapotranspiration (ETc) as a key factor in making informed irrigation decisions, underscoring the significance of accurately determining and spatially mapping crop water status. Technological progress, exemplified by the emergence of unmanned aerial vehicles (UAVs), has brought about a revolutionary shift in agricultural monitoring. UAV platforms can capture high-resolution images with centimeter-level spatial accuracy and offer higher temporal coverage compared to satellite imagery. Considering these advancements, this study introduces a robust method for classifying water stress in cotton using a compact UAV platform and convolutional neural networks (CNN). The experiment was conducted at the USDA-ARS Cropping Systems Research Laboratory (CSRL) in Lubbock, Texas, where the cotton field was divided into 12 drip zones. The study included three replications to evaluate four irrigation treatments: "rainfed", "full irrigation", "percent deficit of full irrigation", and "time delay of full irrigation". The results demonstrated that the CNN model successfully classified the cotton water stress using the UAV-based RGB image, achieving an overall best prediction accuracy of approximately 91%. By segmenting the original cotton images into separate canopy and soil areas using morphological image processing methods, the authors also isolated and analyzed the individual contributions of these components to cotton water stress. Additionally, a random forest classifier revealed the relative importance of different image features in the classification process through feature importance analysis. These findings highlighted the state-of-the-art performance of the proposed system in cotton water stress classification and provided valuable insights into the key image features contributing to accurate classification. The authors concluded that integrating UAV-based RGB imagery and CNN models had great potential for assessing water stress in cotton.

Keywords: cotton; irrigation; water stress; UAV; RGB; evapotranspiration; convolutional neural networks; random forest

1. Introduction

Cotton, accounting for approximately 25% of global fiber usage, is significant among textile fibers worldwide. As the foremost cotton exporter, the United States (US) ranks as the third-largest producer of this vital resource [1]. The northwest plains region of Texas, known as the Texas High Plains (THP), is the largest continuous cotton-producing region of Texas, which contributes to about 25% and 65% of US and Texas cotton production, respectively [2]. While cotton cultivation in THP encompasses dryland and irrigated systems, higher cotton yields are achieved by effectively applying the increased water availability [3]. However, the water resources

are currently insufficient to provide full irrigation in the THP. The Lubbock area, for instance, is facing water limitations because of the significant decline of the water table in the Ogallala Aquifer [4]. Considering the recurring water shortage in THP, finding effective methods to optimize irrigation water use is essential.

In agriculture, evapotranspiration (ET) estimation is one of the most important factors in determining water use efficiency [5], which is defined as the amount of carbon assimilated as biomass or grain produced per unit of water used by the crop [6]. The mapping of ET temporally and spatially can identify variations in the field, which can be used to assess crop water status [7,8]. However, ET estimation of water stress still has some challenges, such as complexity, data requirements, uncertainty, and accuracy [9]. ET estimation methods often require complex calculations and significant data inputs, including meteorological data (temperature, humidity, wind speed, etc.), which can be challenging to collect and may not be readily available [8]. Also, ET estimation models are based on various assumptions and empirical relationships, which can introduce uncertainties and errors in the calculation [10,11]. For a comprehensive exploration of ET research, please refer to the extensive content available in the book authored by Niu and Chen [10].

In recent years, UAVs have emerged as powerful tools for various agricultural applications, including irrigation management [12,13] and water stress estimation [14,15]. With the integration of lightweight sensors on UAV platforms, it has become feasible to capture high-resolution imagery with excellent spatial and temporal resolution at a low cost [16,17]. RGB, thermal, and multispectral cameras are commonly utilized in agricultural research due to their lightweight nature and low power consumption [18,19]. The spatial resolution of UAV-based imagery can reach the centimeter level, which proves valuable in identifying, standardizing, and validating methods for assessing spatial variability in clumped canopy structures such as trees and vines [20]. Numerous studies have demonstrated the potential of UAV imagery for enhancing water stress assessment. For instance, Bian et al. simplified the calculation of the crop water stress index (CWSI) and improved its diagnostic accuracy by employing high-resolution UAV thermal imagery [21]. Zhang et al. showcased the effectiveness of high-resolution UAV RGB images in complementing UAV thermal images for precise extraction of maize canopy temperature [22]. Thermal and RGB orthomosaick were geo-referenced using five ground control points measured using a KOLIDA RTK differential GNSS device. A co-registration approach, the red-green ratio index (RGRI)-Otsu method [22], was used to analyze UAV thermal and RGB images to extract maize canopy temperature at the late vegetative stage. Aversano et al. [23] proposed an automatic end-to-end irrigation system utilizing deep neural networks (DNN) to perform multinomial classification of water stress in tomato plants, based on thermal and optical aerial images. The research findings indicated an average classification accuracy of approximately 80% under optimal hyperparameter conditions.

Building upon prior research, this article proposes the utilization of UAV-based RGB images exclusively for cotton water stress classification, employing convolutional neural networks (CNN). CNNs are highly recognized deep learning architectures comprising input layers, convolution layers, pooling layers, and fully connected layers [24]. Due to their robust analytical capabilities, CNN models have

found applications in various agricultural domains, including yield estimation [25], water stress analysis [26], and pest management [27]. For instance, Yang et al. proposed a CNN model incorporating hyperspectral imagery for corn yield estimation, achieving a classification accuracy of 75.5% using spectral and color image-based integration [28]. Li et al. [27] introduced an efficient data augmentation strategy for pest detection using CNNs. Their approach involved rotating images at different angles and cropping them into multiple grids, resulting in a diverse set of multi-scale examples for training a multi-scale pest detection model. Experimental results showcased an impressive pest detection accuracy of 81.4% through the integration of their data augmentation strategy with the CNN model. Notably, the advancements in CNN models have contributed to significant progress in agricultural research. These examples highlight the potential of UAV-based imagery and its integration with advanced analytical techniques, such as deep neural networks, to enhance water stress analysis and irrigation management in agriculture. By leveraging high-resolution imagery and innovative algorithms, UAVs offer new opportunities for precision agriculture and sustainable water resource management.

The objectives of this study were to: 1) evaluate the reliability of the UAV-based RGB imagery in classifying the cotton water stress with CNN models; 2) demonstrate the performance of the CNN models on irrigation treatment inference; 3) analyze the individual contributions of canopy-only and soil-only images to the cotton water stress with morphological image processing methods; and 4) conduct feature importance analysis using a random forest model. The major contributions of this article were: 1) devised a dependable approach for detecting cotton water stress by utilizing high-resolution RGB images obtained from UAVs and employing CNN models. This approach offered a reliable and efficient solution for monitoring water stress in cotton crops; 2) analyzed the most important features for cotton water stress analysis with random forest classifiers. This analysis helped identify the most significant features for effectively assessing water stress in cotton crops. Understanding the key features contributing to accurate classification enhances our knowledge of the factors influencing water stress in cotton plants.

The rest of the paper is organized as follows: Section 2 offers a comprehensive description of the materials and methods employed for UAV-based irrigation treatment inference. Subsequently, Section 3 presents a thorough analysis and discussion of the obtained results, highlighting the findings related to the reliability of RGB imagery, the performance of CNN models, and the feature importance analysis. Finally, in Section 4, the authors present concluding remarks, summarizing the key insights and implications of the study.

2. Materials and methods

2.1. Experimental site and irrigation management

The study was conducted in an experimental cotton field at the USDA-ARS Cropping Systems Research Laboratory (CSRL) in Lubbock, Texas, USA (33.69° N, 101.82° W). The cotton was planted on 3 May 2022, of the same variety, NG 4098 B3XF, into a full profile using standard planting practices at a rate of 18,500 seeds per hectare (ha). The cotton field was divided into 12 drip zones with three replications to

test 4 irrigation treatments: "rainfed", "full irrigation", "percent deficit of full irrigation", and "time delay of full irrigation" (**Figure 1**). Each drip zone had eight rows. The length of each row was 200 feet, with around 150 cotton plants for each row, and the space between two rows was 40 inches. "Rainfed" treatment relied on pre-plant soil moisture conditions, where the plot was either sown after a planting rainfall or the soil profile was irrigated before sowing on a predetermined date. No additional water was applied during the growing season under this treatment. For the "full irrigation" treatment, irrigation events were triggered by canopy temperature (CT)-based stress time accumulation and the irrigation amount was set to refill the profile based on the accrued moisture deficit. Irrigation occurred as a single event to maintain optimal soil moisture conditions. The "percent deficit of full irrigation" treatment was triggered at a predetermined fraction of the "full irrigation" amount (25%). The frequency of the "percent deficit of full irrigation" was identical to that of "full irrigation", but the irrigation amount was lower. In the "time delay of full irrigation" treatment, irrigation events were triggered every other time the "full irrigation" signal was generated. The irrigation amount was set to completely refill the soil profile, resulting in an approximately 50% decrease in water applied compared to the "full irrigation" treatment. However, longer intervals of water stress were experienced by the cotton under this treatment. To measure the soil moisture, eight soil moisture probes (GoField Plus, Goanna Ag, Goondiwindi QLD, Australia) were installed in different crop rows with one meter depth, located in the four different irrigation treatments. The data was collected every 15 min and reported every hour. The experiment was conducted from May to October 2022. There was no rain before the middle of September.
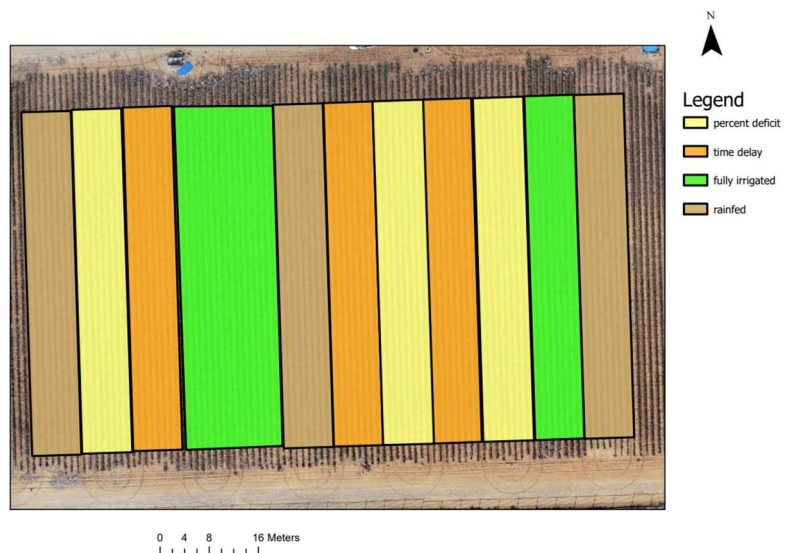

Figure 1. The cotton field experimental layout.

2.2. Description of the UAV and RGB image processing

A DJI Phantom 4 RTK was utilized as the UAV platform for collecting high-resolution RGB images at an altitude of 90 m, with an image resolution of 4096 × 2160. The FC6310R onboard camera features a 1-inch 20-megapixel (MP) complementary metal-oxide semiconductor (CMOS) sensor and a mechanical shutter,

eliminating rolling shutter distortion. This advanced sensor, coupled with impressive processing capabilities, captures intricate detail and provides the image data needed for advanced post-production analysis. Flight missions were conducted biweekly throughout the cotton growing season, spanning from May to October 2022. During each mission, approximately 400 photos were taken. As the sensor flies along a flight path, overlapping images are collected. These images were seamlessly processed together in Metashape (Agisoft LLC, Russian) to produce digital elevation data and orthomosaick. **Figure 2** is an example of the orthomosaick image for 18 August 2022. The orthomosaick generation employs orthorectification, a process that eliminates distortions or displacements in the image caused by factors such as lens distortion, sensor tilt, perspective, and topographic relief. By rectifying these distortions, orthorectification produces a comprehensive and seamless image or map of a specific Earth area, preserving distances accurately, and therefore, the orthomosaick can be used for measurements. The orthomosaick is generated through the creation of a digital surface model (DSM), which in turn is derived from the Densified Point Cloud. This point cloud consists of 3D points generated by matching pixels in image pairs, with these distinct features referred to as key points.
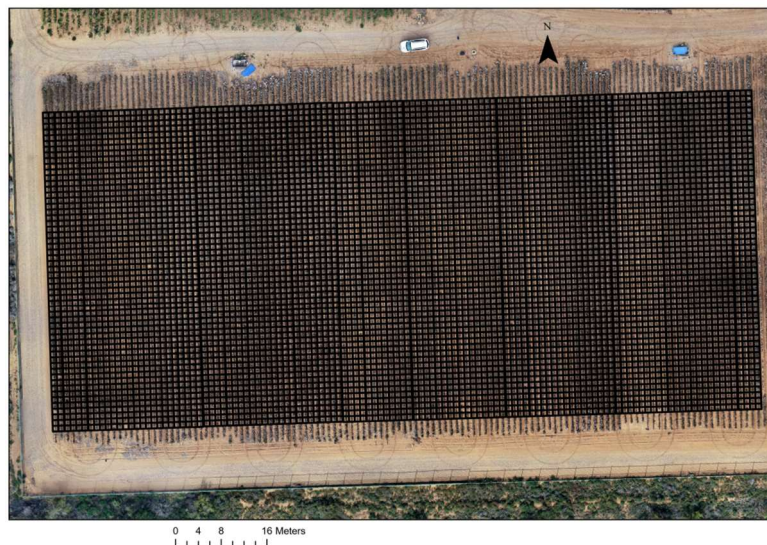

Figure 2. An example of the orthomosaick RGB image for 18 August 2022.

2.3. Cotton segmentation with morphological image processing

The study aimed to classify cotton water stress using advanced CNN models. To effectively analyze the water stress patterns, the authors employed a multi-step approach, taking advantage of both image segmentation and morphological image processing techniques. First, the authors faced the challenge of handling a large-scale UAV cotton image. To address this issue, the authors split the large-scale UAV cotton image into smaller scales with ArcGIS Pro, which created 6832 images for each sampling date, (**Figure 3** is a demonstration of the generated dataset). The new image size was 64 × 64 × 3 (width, height, depth). The ground truth was the irrigation treatment, which was also added at the bottom of each image in **Figure 3** for demonstration. The research goal is to use the CNN model to train the image dataset and classify the image into one of the four irrigation treatments. The term "ground

truth" is crucial in supervised machine learning tasks like image classification. It represents the known and verified correct answers or labels for the data used in training and testing machine learning models. By having this ground truth information, the CNN model can learn from examples and improve its ability to correctly classify images into the specified categories.
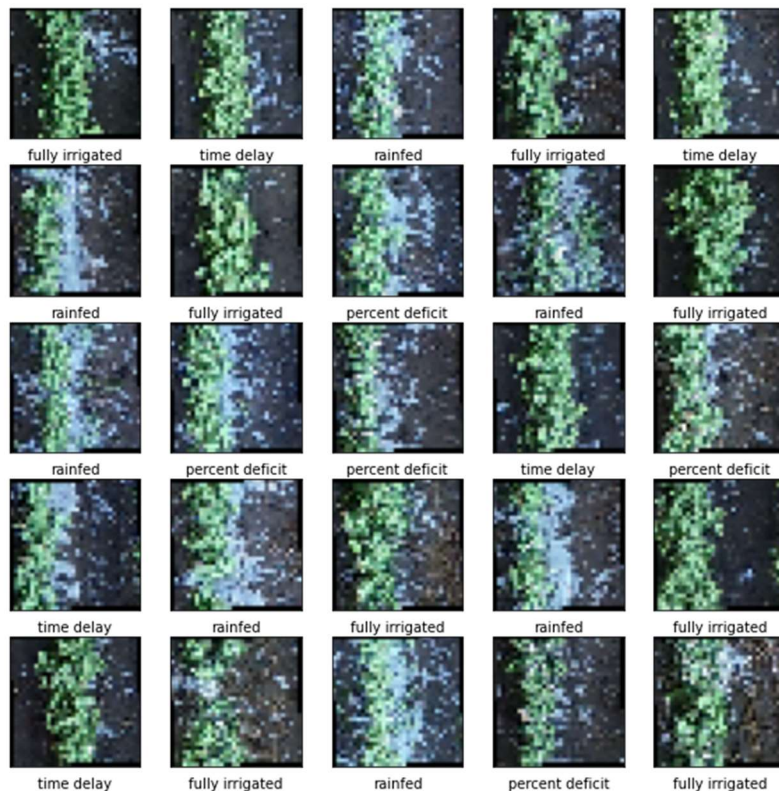

Figure 3. To classify the cotton water stress with CNN models, the authors first split the large scale of the UAV cotton image into smaller scales with ArcGIS Pro, which created 6832 mages for each sampling date.

To further explore the influence of specific factors on water stress prediction, such as the cotton canopy and soil characteristics, the authors turned to morphological image processing methods using scikit-image, an image processing package in Python. Morphological image processing is a fundamental technique for analyzing and manipulating images based on their shape and structure [29]. It is rooted in mathematical morphology, which provides a set of operations for extracting, enhancing, and modifying the geometric features present in an image. These operations are primarily based on the concepts of dilation, erosion, opening, and closing [30]. Dilation expands the shape boundaries and fills gaps, while erosion erodes the boundaries and removes small details. The opening is a combination of erosion followed by dilation, which helps remove noise and small objects. In contrast, closing is a combination of dilation followed by erosion, useful for filling gaps and connecting broken structures [29].

By leveraging morphological image processing techniques, it becomes possible to extract important features, remove noise, segment objects, and perform other essential image analysis tasks, ultimately aiding in the interpretation and

understanding of the cotton image (**Figure 4**). By segmenting the image into cotton and soil areas, the authors could focus on studying the distinct properties and characteristics of each region. This approach enabled a comprehensive analysis of how water stress manifests within the cotton canopy versus the soil, providing valuable insights into the factors influencing water availability and distribution within the field.
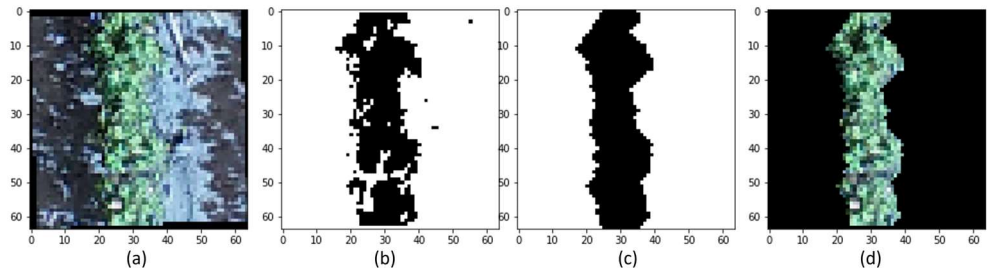

Figure 4. Cotton segmentation with morphological image processing methods. **(a)** the original UAV-based RGB image; **(b)** a rough mask image after Otsu's methods; **(c)** the mask after opening and dilation operations; **(d)** the cotton canopy image with the mask in (c).

To accomplish the task of cotton canopy segmentation, the authors initially converted the RGB image into the LAB color space, which is a color space defined by the International Commission on Illumination (abbreviated CIE) in 1976 [31]. The LAB color space is a color model that represents colors based on three components: L (lightness), A (green-red), and B (blue-yellow). By transforming the RGB image into LAB color space, the authors aimed to exploit the distinctive characteristics of the LAB color channels for better differentiation between the cotton canopy and the background. Because of the green color of the cotton canopy, the authors mainly chose the A channel as the grayscale image for further image processing.

To obtain a rough mask image for cotton canopy segmentation, the authors employed Otsu's method, a widely used technique for automatic thresholding [32]. Otsu's method calculates an optimal threshold value by maximizing the between-class variance of a grayscale image, thus segmenting a grayscale image into two classes: foreground and background. The resulting rough mask image provided an initial segmentation of the cotton canopy region, albeit with some imperfections and noise (**Figure 4b**). This rough mask served as a starting point for further refinement and finetuning of the cotton canopy segmentation process. Subsequent morphological operations, such as opening and dilation, could be applied to improve the accuracy and smoothness of the final mask image (**Figure 4c and 4d**). The conversion of the RGB image into LAB color space and subsequent segmentation of the cotton canopy using morphological image processing techniques provided the authors with a targeted representation of the cotton canopy region. After applying Otsu's method, opening, and dilation operations to generate the mask images, the authors manually assessed the segmentation performance (**Figure 5**). This segmentation step was essential for further analysis and accurate water stress prediction in the cotton field, as it isolated the canopy region from the surrounding background and facilitated the extraction of relevant features for subsequent classification tasks.
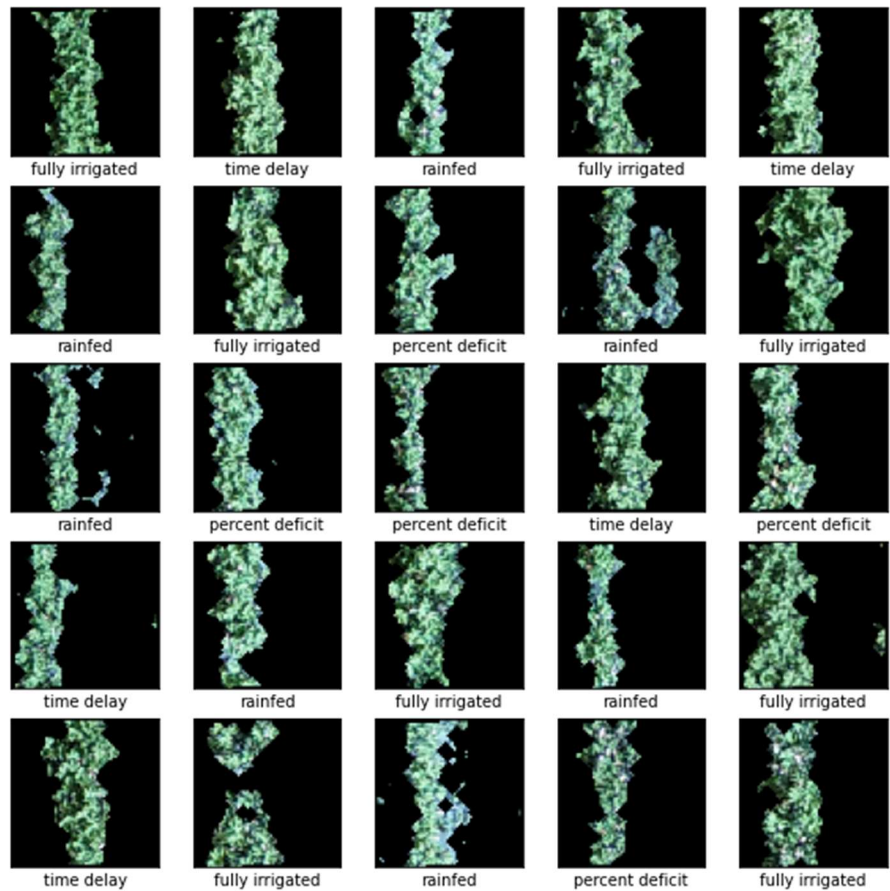
Figure 5. An example of the orthomosaick RGB image for 18 August 2022.

2.4. Image processing for the CNN model

In the data preprocessing stage, the authors divided the large-scale UAV cotton image into smaller scales, resulting in a total of 6832 images for each sampling date. To create a training and testing dataset, the UAV dataset was split into 70% for training and 30% for testing. For visualization, the authors created a plot showcasing the initial 25 images from the training set, with the corresponding class name displayed below each image (**Figure 3**). The TensorFlow 2.0 framework was utilized for implementing the CNN model. The architecture of the CNN model is presented in **Table 1** in the paper. The model primarily consisted of Conv2D and MaxPooling2D layers, with each layer producing a 3D tensor output representing height, width, and channels. As the network went deeper, the width and height dimensions tended to decrease. The number of output channels for each Conv2D layer was determined by the first argument specified. The output tensor generated from the convolutional base was then fed into Dense layers for classification. Given that the dataset comprised four irrigation treatments, the final Dense layer had four outputs, enabling the model to classify the input images into the respective treatment categories. This architecture ensured that the model effectively learned and distinguished between the different irrigation treatments based on the provided training data. Parameter tuning is a crucial step in the process of building the CNN model, as it involves finding the optimal configuration of hyperparameters to enhance the model's performance. Hyperparameters are external configurations that cannot be learned from the data and

significantly influence the model's behavior. In the context of the CNN model, hyperparameters include values such as the number of neurons in layers, kernel sizes in convolutional layers, and the choice of optimizer algorithms. Automated tools, libraries, and frameworks, such as scikit-learn, and TensorFlow, provide convenient ways to perform systematic hyperparameter tuning, contributing to the development of more accurate and robust machine learning or deep learning models. In this article, parameters were searched in the following parameter grid: {'optimizer': ['adam', 'sgd'], 'neurons': [32, 64, 128], 'kernel_size': [(3, 3), (4, 4)], 'pool_size': [(2, 2), (3, 3)]}. It turned out that the architecture shown in **Table 1**. had the best model performance for our validation. The CNN model utilized in this study can be easily reproduced for validation purposes. For more comprehensive information and specific instructions on replicating the model, please refer to the "Reproducibility" section located at the end of the paper.

Table 1. The architecture of the CNN model.

Layer type	Output shape	Parameter numbers
Conv2D	(None, 62, 62, 32)	896
MaxPooling2D	(None, 31, 31, 32)	0
Conv2D	(None, 29, 29, 64)	18496
MaxPooling2D	(None, 14, 14, 64)	0
Conv2D	(None, 12, 12, 64)	36928
Flatten	(None, 9216)	0
Dense	(None, 64)	589888
Dense	(None, 4)	260

2.5. Cotton canopy cover analysis

According to Ashapure [33], canopy cover is typically quantified as the percentage of ground area covered by the vertical projection of the plant canopy. This parameter is closely associated with crop growth, development, water utilization, and photosynthesis, rendering it a significant characteristic that necessitates continuous monitoring throughout the growing season [34]. Monitoring the cotton canopy cover through the growing season can provide valuable insights into the overall performance of the cotton. To gain a comprehensive understanding of cotton growth during the growing season in 2022, the authors analyzed the canopy cover trends, an important indicator of cotton growth. The canopy cover was calculated with the same method shown in the study of Ashapure et al. [35]. The RGB orthomosaick image was first classified into a binary map using the Canopeo algorithm [36]. Then, Equations (1) and (2) were applied to compute the canopy cover.

$$canopy = \left(\frac{red}{green} < p_1\right) \text{ and } \left(\frac{blue}{green} < p_2\right) \text{ and } (2green - blue - red > p_3) \quad (1)$$

where red, green, and blue were the pixel values in the corresponding band. The parameters p_1, p_2, and p_3 were used to classify pixels that were predominantly in the green band [37,38]. The default values for the Canopeo algorithm were $p_1 = 0.95$, $p_2 = 0.95$, and $p_3 = 20$ [36].

$$\text{canopy cover} = \frac{\Sigma(GSD^2) \text{ if canopy}}{\Sigma(GSD^2)} \qquad (2)$$

where GSD is the ground sample distance. The GSD was the distance between two consecutive pixel centers measured on the ground [35].

2.6. Feature importance analysis

In the feature importance analysis, the random forest classifier was trained on the same dataset used for training the CNN model (the dataset on August 18th). The random forest algorithm is a powerful machine-learning technique that can provide insights into the importance of different input features for making accurate predictions [39]. It works by constructing a multitude of decision trees and averaging their predictions to produce a final classification result. This analysis is based on evaluating the impact of each feature on the reduction of impurity within decision trees. For the random forest algorithm, the default setting of sklearn.ensemble.RandomForestClassifier from scikit-learn was applied for feature importance analysis. The code was attached in the appendix, where parameters are shown with the RandomForestClassifier().get_params() function. Compared with 'activation maps' or 'gradient-based' methods, the use of Random Forest for feature importance analysis is particularly beneficial in scenarios where interpretability and transparency are essential. In contrast, 'activation maps' and 'gradient-based' methods often involve complex computations and may provide less straightforward interpretations of feature importance. For example, random forest provides a highly interpretable way to assess feature importance. The ensemble of decision trees allows for a clear understanding of how each feature contributes to the overall prediction. While activation maps or gradient-based methods can provide insights into which regions of the input contribute to the output, the interpretation might not be as intuitive as the feature importance scores provided by random forests. Therefore, feature importance analysis using the random forest is preferred for the cotton water stress applications in this article.

For the cotton water stress task, 8 features were derived from the UAV-based RGB image, which was "red", "green", "blue", "exgreeness", "canopy cover", "canopy volume", "mask size", and "canopy height". The "red", "green", and "blue" were mean band reflectance values for the cotton canopy area. The "exgreeness" represented the excess green index (EXGI). The EXGI contrasts the green portion of the spectrum against red and blue to distinguish vegetation from soil and can also be used to predict NDVI values. It has been shown to outperform other indices that work with the visible spectrum to distinguish vegetation [40]. The EXGI was computed by Equation (3):

$$EXGI = 2G - (R + B) \qquad (3)$$

where G, R, and B are normalized green, red, and blue bands, respectively [35]. The canopy volume was calculated by Equation (4):

$$\text{canopy volume} = \Sigma(H_i \times GSD^2) \qquad (4)$$

where H_i is the height of the ith pixel [35]. The Canopy height calculation was obtained from the CHM (canopy height model). The CHM is generated by subtracting the DSM of each flight from the digital terrain model (DTM) obtained during the first flight.

The first flight was conducted after planting and prior to plant emergence to obtain the bare earth surface without any features, such as vegetation.

3. Results and discussion

3.1. Overall cotton growing trends

The irrigation treatment played a vital role in cotton growth, and its impact on cotton canopy cover was evaluated based on the amount, frequency, and timing of water application (**Figure 6**). The "rainfed" treatment resulted in reduced canopy cover, as cotton conserved water by reducing its leaf area or closing its stomata to minimize water loss. Similar effects of reduced irrigation on canopy cover and leaf area were observed in a previous study on drip-irrigated blueberries [41]. Conversely, the fully irrigated treatment led to excessive canopy cover, as cotton plants responded to the surplus water supply by producing more leaves. However, excessive growth of canopy cover may also lead to decreased water use efficiency, increased susceptibility to disease, and compromised fruit quality [42]. Therefore, applying water at the appropriate amount and timing, based on the specific water requirements of the plants, is crucial for achieving optimal canopy cover and promoting healthy plant growth.
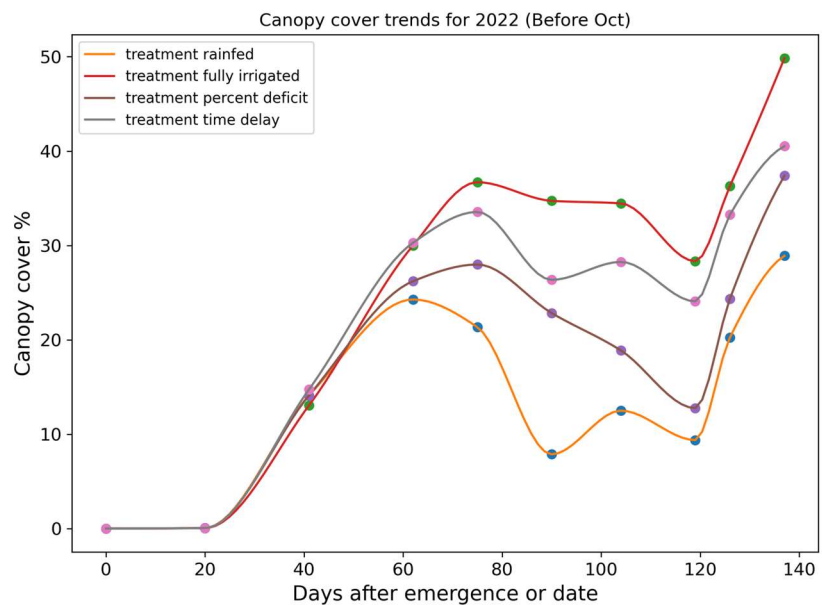

Figure 6. The cotton canopy covers trends. Irrigation treatments played a vital role in cotton growth, and their impact on cotton canopy cover was evaluated based on the amount, frequency, and timing of water application.

Notably, one of the key research findings was the significant differences observed among the irrigation treatments during the middle of the growing season, specifically between 60 and 120 days after the emergence (primarily in August and September 2022). This period marked a critical stage where the divergent effects of different irrigation treatments on canopy cover became more pronounced. Understanding these variations and their implications during this specific timeframe provided valuable insights into the optimal management of irrigation practices for cotton cultivation.

Considering the importance of this specific stage, the subsequent section of the study focused primarily on utilizing the dataset collected during August and September for training and testing the CNN models. By concentrating on this specific period, the authors aimed to capture and analyze the key features and patterns related to cotton growth that emerged during these critical months. This targeted approach allowed for a more in-depth exploration of the effects of irrigation treatments on cotton growth and provided valuable data for training and evaluating the CNN models.

3.2. The performance of the CNN model

The study utilized a total of 6832 cotton canopy images for each sampling date: Aug 18th, Sep 2nd, Sep 9th, and Sep 20th, all in 2022. For each sampling day, the dataset was randomly split into a 70% training set and a 30% testing. During the training process, the CNN model was trained using the "Adam" optimizer and the cross-entropy loss function. The model was trained for a total of 70 epochs, with the aim of optimizing its performance. To assess the performance of the trained CNN models, the authors employed the original dataset (**Figure 3**) and plotted the training and testing accuracy curves as the number of epochs increased (**Figure 7**). The test accuracy achieved varied for each sampling date, with approximately 91% for Aug 18th, 85% for Sep 2nd, 86% for Sep 9th, and 71% for Sep 20th in 2022. These accuracy values provided insights into the performance of the CNN models in classifying cotton water stress levels on different sampling dates.
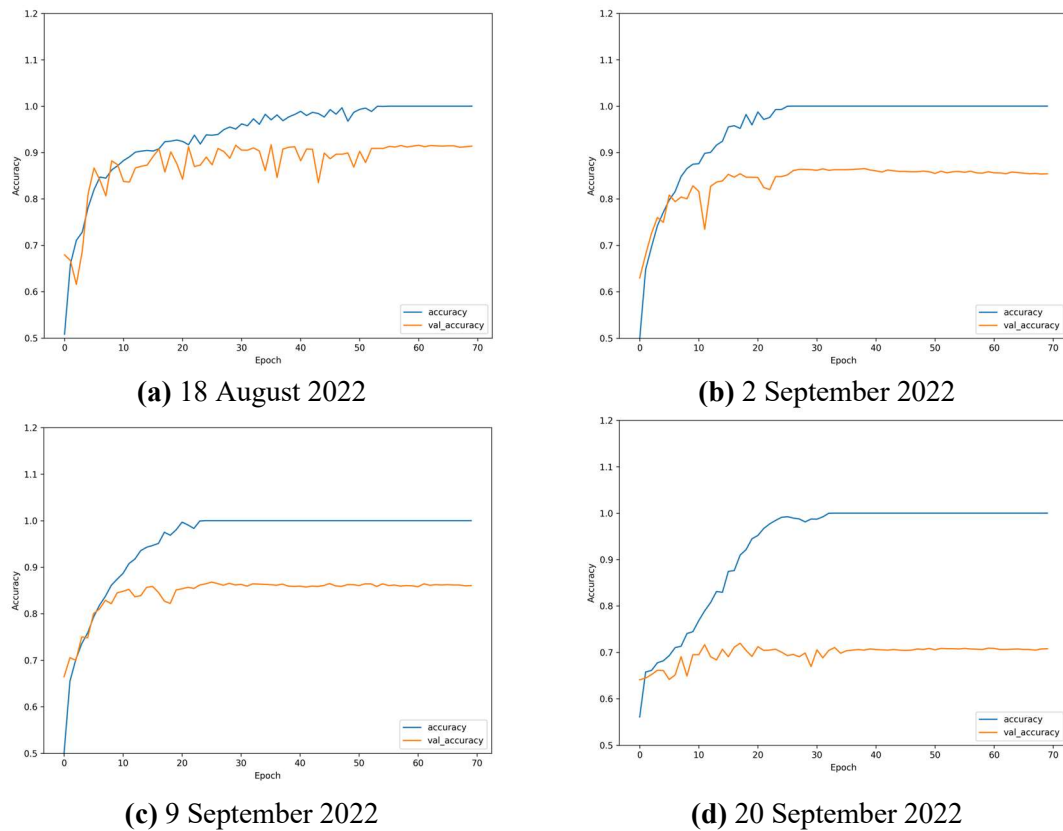

(a) 18 August 2022

(b) 2 September 2022

(c) 9 September 2022

(d) 20 September 2022

Figure 7. The training and testing accuracy of the CNN model for the original image dataset at different sampling days.

To evaluate the performance of the trained CNN models, the authors employed a confusion matrix, which provided a comprehensive summary of the prediction results in a classification problem. The confusion matrix helped in understanding not only the overall accuracy of the classifier but also the specific types of errors being made. In this study, the confusion matrix was utilized to assess the CNN model's performance in predicting the irrigation treatment levels. The "True label" in the confusion matrix represented the actual irrigation treatment levels based on the ground truth data. On the other hand, the "Predicted label" indicated the irrigation treatment levels predicted by the trained CNN model. To simplify the visualization, the irrigation treatments were labeled numerically as follows: "rainfed" as "0", "fully irrigated" as "1", "percent deficit" as "2", and "time delay" as "3" (**Figure 8**). The color bar on the right side of the confusion matrix represents the number of test samples.

(a) Aug 18th, 2022.

(b) Sep 2nd, 2022.

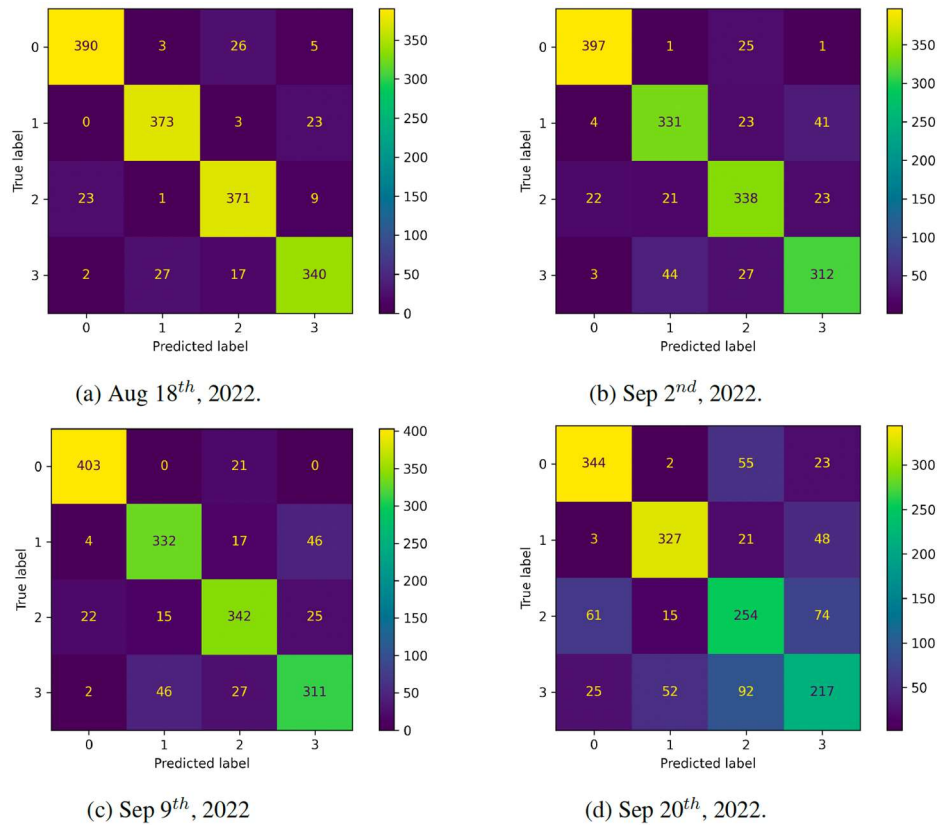(c) Sep 9th, 2022

(d) Sep 20th, 2022.

Figure 8. Summary of prediction results of the CNN model for the original image dataset at different sampling days. The irrigation treatments were labeled as follows: "rainfed" as "0", "fully irrigated" as "1", "percent deficit" as "2", and "time delay" as "3". The color bar on the right side shows the test samples.

To provide more detailed information on the model's performance, precision and recall values were calculated and presented in **Table 2.** Precision measures the proportion of correctly predicted samples for each class, while recall measures the proportion of correctly predicted samples out of all the samples that belong to a particular class. These metrics provide valuable insights into the model's accuracy and ability to correctly classify different irrigation treatment levels. The test accuracy achieved was approximately 91% for Aug 18th, 85% for Sep 2nd, 86% for Sep 9th,

and 71% for Sep 20th in 2022. The lower performance observed on the last sampling date (Sep 20th) could be attributed to several factors. One of the important reasons was that rainfall happened before Sep 20th. As the cotton plants progressed in their growth cycle, the canopy structure and appearance changed compared to earlier sampling dates. The canopy cover increased significantly compared with the previous sampling dates (**Figure 6**). This change in canopy characteristics could have introduced additional variability and complexity in the UAV-based RGB images, making it more challenging for the CNN models to accurately classify them. These factors could affect the overall health and vitality of the cotton, potentially leading to variations in their visual appearance and making classification more difficult [43].

Table 2. The CNN model's classification performance on irrigation treatments for each sampling day (original image dataset).

Date	Irrigation treatments	Precision	Recall	F1-score
Aug 18th	rainfed	0.94	0.92	0.93
Aug 18th	fully irrigated	0.92	0.93	0.93
Aug 18th	percent deficit	0.89	0.92	0.90
Aug 18th	time delay	0.90	0.88	0.89
Sep 2nd	rainfed	0.93	0.94	0.93
Sep 2nd	fully irrigated	0.83	0.83	0.83
Sep 2nd	percent deficit	0.82	0.84	0.83
Sep 2nd	time delay	0.83	0.81	0.82
Sep 9th	rainfed	0.94	0.95	0.94
Sep 9th	fully irrigated	0.84	0.83	0.84
Sep 9th	percent deficit	0.84	0.85	0.84
Sep 9th	time delay	0.81	0.81	0.81
Sep 20th	rainfed	0.79	0.81	0.80
Sep 20th	fully irrigated	0.83	0.82	0.82
Sep 20th	percent deficit	0.60	0.63	0.62
Sep 20th	time delay	0.60	0.56	0.58

3.3. Canopy-only and soil-only images for cotton water stress analysis

The utilization of canopy-only and soil-only images in cotton water stress analysis serves a specific purpose and offers valuable insights into the underlying factors affecting plant health and water needs. By segmenting the original cotton canopy images into separate canopy and soil areas using morphological image processing methods, the authors aimed to isolate and analyze the individual contributions of these components to cotton water stress.

The canopy cover plays a crucial role in determining water requirements and overall plant health [44]. It directly influences factors such as transpiration, photosynthesis, and evaporation rates, which are vital indicators of water stress levels in cotton plants. By examining the canopy-only images (**Figure 5**), the authors can focus on assessing the extent and distribution of canopy coverage, as well as detecting any signs of wilting, senescence, or other stress-related symptoms. These observations

enable a more accurate evaluation of the impact of water availability and irrigation treatments on the cotton canopy.

On the other hand, analyzing the soil-only images provides crucial information about the moisture content. Soil moisture directly affects the plant's ability to extract water and nutrients, impacting its overall water status. By examining the soil-only images, the authors can assess the spatial variability of soil moisture and its relationship to irrigation treatments. This analysis helps understand how different irrigation strategies influence soil moisture levels and the subsequent impact on cotton water stress. To generate the soil-only images, the authors simply inverted the binary image mask created for the canopy-only images (**Figure 5**), resulting in a visual representation of the soil in the cotton field.

Then, the same CNN model was employed for training and testing the canopy-only and soil-only images. To provide a comprehensive understanding of the model's performance, precision and recall values were calculated and presented in **Table 3**. In the table, the authors presented the classification performance for both the canopy-only and soil-only images together. For example, "Accuracy (Canopy/Soil)" indicated that the overall accuracy of the canopy-only image dataset was on the left, while the overall accuracy of the soil-only image dataset was displayed on the right.

Table 3. The CNN model's classification performance on irrigation treatments for each sampling day (canopy-only and soil-only image datasets).

Date	Irrigation treatments	Precision (canopy/soil)	Recall (canopy/soil)	F1-score (canopy/soil)
Aug 18th	rainfed	0.86/0.83	0.84/0.87	0.85/0.85
Aug 18th	fully irrigated	0.90/0.82	0.90/0.82	0.90/0.82
Aug 18th	percent deficit	0.79/0.65	0.80/0.64	0.80/0.65
Aug 18th	time delay	0.84/0.67	0.84/0.66	0.84/0.66
Sep 2nd	rainfed	0.79/0.88	0.82/0.90	0.81/0.89
Sep 2nd	fully irrigated	0.73/0.77	0.67/0.72	0.70/0.74
Sep 2nd	percent deficit	0.62/0.74	0.65/0.74	0.63/0.74
Sep 2nd	time delay	0.64/0.69	0.63/0.74	0.63/0.71
Sep 9th	rainfed	0.78/0.89	0.82/0.90	0.80/0.90
Sep 9th	fully irrigated	0.70/0.78	0.68/0.72	0.69/0.75
Sep 9th	percent deficit	0.63/0.76	0.63/0.76	0.63/0.76
Sep 9th	time delay	0.63/0.71	0.61/0.75	0.62/0.73
Sep 20th	rainfed	0.72/0.76	0.73/0.76	0.72/0.76
Sep 20th	fully irrigated	0.78/0.78	0.73/0.76	0.75/0.77
Sep 20th	percent deficit	0.53/0.53	0.52/0.54	0.52/0.54
Sep 20th	time delay	0.50/0.53	0.54/0.54	0.52/0.54

As anticipated, the CNN performance for these individual image subsets did not surpass the performance achieved with the original UAV-based RGB image dataset, as indicated in **Table 2**. Another notable research finding was that the irrigation treatments "rainfed" and "fully irrigated" were relatively easier to classify compared with the other two irrigation treatments. This observation could be attributed to several

factors. The CNN model relied on patterns and features present in the input data to make accurate predictions. By using only the canopy or soil images, certain contextual information that could be captured in the original RGB image may be omitted. The RGB image captured not only the individual components of the plant and soil but also their interactions, which could provide additional cues for accurate classification.

3.4. Feature importance analysis

In the above discussion, it can be concluded that the CNN model demonstrates state-of-the-art performance in cotton water stress classification. However, a limitation lies in the lack of physiological interpretability, specifically the understanding of which features contributed to the classification tasks. To address this limitation and gain further insights into the classification performance, the authors conducted a feature importance analysis using the random forest classifier.

The classification performance of the random forest model is shown in **Table 4**. After training the random forest classifier, the authors computed the feature importance scores based on the Gini impurity index. The Gini impurity measured the extent of impurity or disorder in a node of a decision tree, and the feature importance score represented the reduction in Gini impurity achieved by splitting on a particular feature [45]. Higher feature importance scores indicated that the corresponding feature played a more significant role in the classification task. The feature importance analysis results are shown in **Figure 9**.

Table 4. The random forest classifier performance.

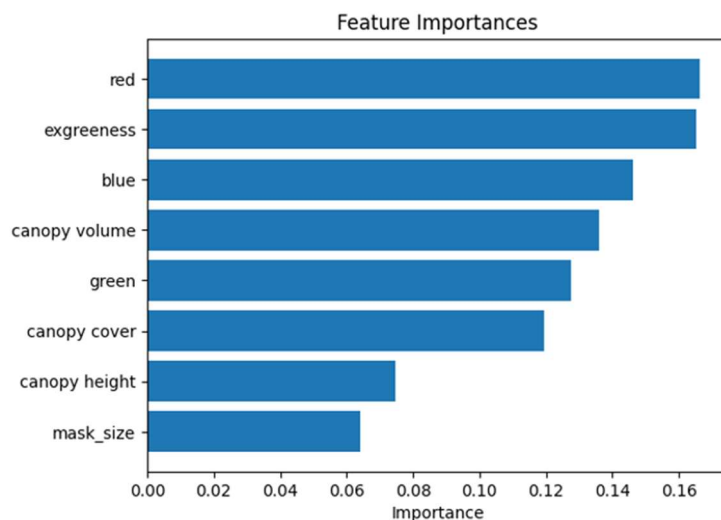| Irrigation treatment	Precision	Recall	F1-score
rainfed	0.93	0.96	0.94
fully irrigated	0.94	0.96	0.95
percent deficit	0.93	0.90	0.92
time delay	0.94	0.92	0.93
accuracy			0.93

Figure 9. Feature importance analysis results. Higher feature importance scores indicated that the corresponding feature played a more significant role in the classification task.

The high feature importance score for the "red" channel indicated that it carried significant information for accurately classifying cotton water stress levels. The red channel represented the intensity of the red color component in the image, which was closely related to the absorption and reflection properties of vegetation. In the context of cotton water stress analysis, the red channel could provide valuable insights into the physiological changes in the cotton canopy. As water stress increases, plants typically undergo physiological adjustments that affect their pigment concentration and chlorophyll content [46,47]. These changes could alter the reflectance properties of the plant, particularly in the red portion of the spectrum. Therefore, the red channel became a relevant indicator for detecting variations in water stress levels.

By analyzing the feature importance scores, the authors gained valuable insights into the key factors that contributed to the accurate classification of cotton water stress. These insights could provide a better understanding of the physiological and environmental factors that drove variations in cotton water stress levels. Additionally, the feature importance analysis helped identify the most informative features for future monitoring and assessment of cotton water stress, potentially enabling more targeted and efficient management practices.

4. Conclusion

In this article, the authors demonstrate the effectiveness of using a CNN model for cotton water stress classification with state-of-the-art performance. By training the model on a large dataset of UAV-based RGB images, the authors achieved high accuracy (91%) in distinguishing between different irrigation treatments. The analysis of canopy-only and soil-only images provided valuable insights into the individual contributions of canopy cover and soil moisture to water stress assessment. However, the CNN model's performance using these individual image subsets did not surpass the performance achieved with the original RGB image dataset. This suggested that the CNN model benefited from the contextual information and interactions captured in the RGB images. Additionally, the feature importance analysis using a random forest classifier revealed the significant contributions of specific image features, such as the red and blue channels, canopy cover, and other vegetation characteristics.

This knowledge can inform future research on the physiological mechanisms underlying cotton water stress and guide the development of more targeted water management strategies. For example, cotton water stress is influenced by various environmental factors, including temperature, humidity, and solar radiation. Investigating the integration of environmental data alongside RGB imagery can improve the accuracy of water stress classification models by considering the contextual effects of these factors. Training CNN models on larger and more diverse datasets, encompassing different regions and cultivars, can enhance model generalization capabilities. Additionally, applying transfer learning techniques to pre-training models on related crops or plant species may help improve the performance of cotton water stress classification. Overall, the study highlights the potential of deep learning models to advance our understanding and monitoring of crop water stress for improved agricultural practices. The authors concluded that the integration of UAV-based RGB imagery and CNN models had great potential for assessing water stress in

cotton.

Appendix: Research reproducibility: All the research results in this article can be reproduced. The code and dataset are available on the author's Github: https://github.com/hniu-tamu/cotton_water_stress_remote_sensing.

References

1. Johnson J, Kiawu J, Macdonald S, et al. The world and United States cotton outlook. Available online: http://ageconsearch.umn.edu (accessed on 2 December 2023).
2. Adhikari P, Ale S, Bordovsky JP, et al. Simulating future climate change impacts on seed cotton yield in the Texas High Plains using the CSM-CROPGRO-Cotton model. Agricultural Water Management. 2016, 164: 317-330. doi: 10.1016/j.agwat.2015.10.011
3. Ale S, Himanshu SK, Mauget SA, et al. Simulated Dryland Cotton Yield Response to Selected Scenario Factors Associated with Soil Health. Frontiers in Sustainable Food Systems. 2021, 4. doi: 10.3389/fsufs.2020.617509
4. Bordovsky JP, Mustian JT, Ritchie GL, Lewis KL. Cotton irrigation timing with variable seasonal irrigation capacities in the Texas South Plains. Applied Engineering in Agriculture. 2015, 31(6): 883-897. doi: 10.13031/aea.31.10953
5. Allen RG, Pereira LS. Crop evapotranspiration (guidelines for computing crop water requirements). Available online: https://www.fao.org/3/x0490e/x0490e00.htm (accessed on 2 December 2023).
6. Hatfield JL, Dold C. Water-Use Efficiency: Advances and Challenges in a Changing Climate. Frontiers in Plant Science. 2019, 10. doi: 10.3389/fpls.2019.00103
7. Kaplan S, Myint SW, Fan C, et al. Quantifying Outdoor Water Consumption of Urban Land Use/Land Cover: Sensitivity to Drought. Environmental Management. 2014, 53(4): 855-864. doi: 10.1007/s00267-014-0245-7
8. Niu H, Hollenbeck D, Zhao T, et al. Evapotranspiration Estimation with Small UAVs in Precision Agriculture. Sensors. 2020, 20(22): 6427. doi: 10.3390/s20226427
9. Gowda PH, Chavez JL, Colaizzi PD, et al. ET mapping for agricultural water management: present status and challenges. Irrigation Science. 2007, 26(3): 223-237. doi: 10.1007/s00271-007-0088-6
10. Niu H, Chen Y. Towards Tree-Level Evapotranspiration Estimation with Small UAVs in Precision Agriculture. Springer International Publishing; 2022. doi: 10.1007/978-3-031-14937-5
11. Zhao WL, Qiu GY, Jiu YX, et al. Uncertainties caused by resistances in evapotranspiration estimation using high-density eddy covariance measurements. Journal of Hydrometeorology. 2020, 21(6): 1349–1365. doi: 10.1175/JHM-D-19-0191.1
12. Niu H, Zhao T, Wang D, et al. A UAV resolution and waveband aware path planning for onion irrigation treatments inference. In: Proceedings of the 2019 International Conference on Unmanned Aircraft Systems (ICUAS); 11–14 June 2019; Atlanta, GA, USA. pp. 808–812. doi: 10.1109/icuas.2019.8798188

13. Zhao T, Wang D, Niu H, et al. Onion irrigation treatment inference using a low-cost hyperspectral scanner. In: Proceedings of the Multispectral, Hyperspectral, and Ultraspectral Remote Sensing Technology, Techniques and Applications VII; 24–26 September 2018; Honolulu, Hawaii, United States. doi: 10.1117/12.2325500

14. Zhao T, Chen Y, Ray A, et al. Quantifying almond water stress using unmanned aerial vehicles (UAVs): Correlation of stem water potential and higher order moments of non-normalized canopy distribution. In: Proceedings of the 13th ASME/IEEE International Conference on Mechatronic and Embedded Systems and Applications; 6–9 August 2017; Cleveland, Ohio, USA. doi: 10.1115/detc2017-68246

15. Zhang L, Zhang H, Niu Y, et al. Mapping Maize Water Stress Based on UAV Multispectral Remote Sensing. Remote Sensing. 2019, 11(6): 605. doi: 10.3390/rs11060605

16. Khanal S, Fulton J, Shearer S. An overview of current and potential applications of thermal remote sensing in precision agriculture. Computers and Electronics in Agriculture. 2017, 139: 22-32. doi: 10.1016/j.compag.2017.05.001

17. Viers J, Niu H, Zhao T, et al. A detailed study on accuracy of uncooled thermal cameras by exploring the data collection workflow. In: Autonomous Air and Ground Sensing Systems for Agricultural Optimization and Phenotyping III. SPIE; 2018. doi: 10.1117/12.2305217

18. Hoffmann H, Nieto H, Jensen R, et al. Estimating evaporation with thermal UAV data and two-source energy balance models. Hydrology and Earth System Sciences. 2016, 20(2): 697-713. doi: 10.5194/hess-20-697-2016

19. Ribeiro-Gomes K, Hernández-López D, Ortega J, et al. Uncooled Thermal Camera Calibration and Optimization of the Photogrammetry Process for UAV Applications in Agriculture. Sensors. 2017, 17(10): 2173. doi: 10.3390/s17102173

20. Niu H, Zhao T, Wei J, et al. Reliable tree-level evapotranspiration estimation of pomegranate trees using lysimeter and UAV multispectral imagery. In: Proceedings of the 2021 IEEE Conference on Technologies for Sustainability (SusTech); 22–24 April 2021; Irvine, CA, USA. pp. 1–6. doi: 10.1109/sustech51236.2021.9467413

21. Bian J, Zhang Z, Chen J, et al. Simplified Evaluation of Cotton Water Stress Using High Resolution Unmanned Aerial Vehicle Thermal Imagery. Remote Sensing. 2019, 11(3): 267. doi: 10.3390/rs11030267

22. Zhang L, Niu Y, Zhang H, et al. Maize Canopy Temperature Extracted from UAV Thermal and RGB Imagery and Its Application in Water Stress Monitoring. Frontiers in Plant Science. 2019, 10. doi: 10.3389/fpls.2019.01270

23. Aversano L, Bernardi ML, Cimitile M. Water stress classification using Convolutional Deep Neural Networks. JUCS - Journal of Universal Computer Science. 2022, 28(3): 311-328. doi: 10.3897/jucs.80733

24. LeCun Y, Bengio Y, Hinton G. Deep learning. Nature. 2015, 521(7553): 436-444. doi: 10.1038/nature14539

25. Khaki S, Wang L, Archontoulis SV. A CNN-RNN Framework for Crop Yield Prediction. Frontiers in Plant Science. 2020, 10. doi: 10.3389/fpls.2019.01750

26. Chandel NS, Chakraborty SK, Rajwade YA, et al. Identifying crop water stress using deep learning models. Neural Computing and Applications. 2020, 33(10): 5353-5367. doi: 10.1007/s00521-020-05325-4

27. Li R, Jia X, Hu M, et al. An Effective Data Augmentation Strategy for CNN-Based Pest Localization and Recognition in the Field. IEEE Access. 2019, 7: 160274-160283. doi: 10.1109/access.2019.2949852

28. Yang W, Nigon T, Hao Z, et al. Estimation of corn yield based on hyperspectral imagery and convolutional neural network. Computers and Electronics in Agriculture. 2021, 184: 106092. doi: 10.1016/j.compag.2021.106092

29. Gonzalez RC, Woods RE, Eddins SL. Digital Image Processing Using MATLAB, 3rd ed. Gatesmark Publishing; 2020.

30. Szeliski R. Computer Vision. Springer International Publishing; 2022. doi: 10.1007/978-3-030-34372-9

31. Billmeyer FW. Color Science: Concepts and Methods, Quantitative Data and Formulae, 2nd ed., by Gunter Wyszecki and W. S. Stiles, John Wiley and Sons, New York, 1982, 950 pp. Price: $75.00. Color Research & Application. 1983, 8(4): 262-263. doi: 10.1002/col.5080080421

32. Otsu N. A Threshold Selection Method from Gray-Level Histograms. IEEE Transactions on Systems, Man, and Cybernetics. 1979, 9(1): 62-66. doi: 10.1109/tsmc.1979.4310076

33. Ashapure A, Jung J, Chang A, et al. A Comparative Study of RGB and Multispectral Sensor-Based Cotton Canopy Cover Modelling Using Multi-Temporal UAS Data. Remote Sensing. 2019, 11(23): 2757. doi: 10.3390/rs11232757

34. Trout TJ, Johnson LF, Gartung J. Remote Sensing of Canopy Cover in Horticultural Crops. HortScience. 2008, 43(2): 333-337. doi: 10.21273/hortsci.43.2.333

35. Ashapure A, Jung J, Chang A, et al. Developing a machine learning based cotton yield estimation framework using multi-temporal UAS data. ISPRS Journal of Photogrammetry and Remote Sensing. 2020, 169: 180-194. doi: 10.1016/j.isprsjprs.2020.09.015

36. Patrignani A, Ochsner TE. Canopeo: A Powerful New Tool for Measuring Fractional Green Canopy Cover. Agronomy Journal. 2015, 107(6): 2312-2320. doi: 10.2134/agronj15.0150

37. Meyer GE, Neto JC. Verification of color vegetation indices for automated crop imaging applications. Computers and Electronics in Agriculture. 2008, 63(2): 282-293. doi: 10.1016/j.compag.2008.03.009

38. Paruelo JM, Lauenroth WK, Roset PA. Estimating Aboveground Plant Biomass Using a Photographic Technique. Journal of Range Management. 2000, 53(2): 190. doi: 10.2307/4003281

39. Pal M. Random Forest classifier for remote sensing classification. International Journal of Remote Sensing. 2005, 26(1): 217-222. doi: 10.1080/01431160412331269698

40. Larrinaga A, Brotons L. Greenness Indices from a Low-Cost UAV Imagery as Tools for Monitoring Post-Fire Forest Recovery. Drones. 2019, 3(1): 6. doi: 10.3390/drones3010006

41. Ortega-Farias S, Espinoza-Meza S, López-Olivari R, et al. Effects of different irrigation levels on plant water status, yield, fruit quality, and water productivity in a drip-irrigated blueberry orchard under Mediterranean conditions. Agricultural Water Management. 2021, 249: 106805. doi: 10.1016/j.agwat.2021.106805

42. Zhang D, Liu Y, Li Y, et al. Reducing the Excessive Evaporative Demand Improved the Water-use Efficiency of Greenhouse Cucumber by Regulating the Trade-off between Irrigation Demand and Plant Productivity. HortScience. 2018, 53(12): 1784-1790. doi: 10.21273/hortsci13129-18

43. Tarara JM, Perez Peña JE. Moderate Water Stress from Regulated Deficit Irrigation Decreases Transpiration Similarly to Net Carbon Exchange in Grapevine Canopies. Journal of the American Society for Horticultural Science. 2015, 140(5): 413-426. doi: 10.21273/jashs.140.5.413

44. Morales-Santos A, Nolz R. Assessment of canopy temperature-based water stress indices for irrigated and rainfed soybeans under subhumid conditions. Agricultural Water Management. 2023, 279: 108214. doi: 10.1016/j.agwat.2023.108214

45. Yuan Y, Wu L, Zhang X. Gini-Impurity Index Analysis. IEEE Transactions on Information Forensics and Security. 2021, 16: 3154-3169. doi: 10.1109/tifs.2021.3076932

46. Ballester C, Brinkhoff J, Quayle WC, et al. Monitoring the Effects of Water Stress in Cotton using the Green Red Vegetation Index and Red Edge Ratio. Remote Sensing. 2019, 11(7): 873. doi: 10.3390/rs11070873

47. Tong A, He Y. Estimating and mapping chlorophyll content for a heterogeneous grassland: Comparing prediction power of a suite of vegetation indices across scales between years. ISPRS Journal of Photogrammetry and Remote Sensing. 2017, 126: 146-167. doi: 10.1016/j.isprsjprs.2017.02.010